Thermopower of a one-dimensional ballistic constriction in the non-linear regime

1993 J. Phys.: Condens. Matter 5 8055

(http://iopscience.iop.org/0953-8984/5/43/017)

J. Phys.: Condens. Matter 5 (1993) 8055–8064. Printed in the UK

Thermopower of a one-dimensional ballistic constriction in the non-linear regime

A S Dzurak†, C G Smith†, L Martín-Moreno†§, M Pepper†‡, D A Ritchie†, G A C Jones† and D G Hasko†

† Cavendish Laboratory, Madingley Road, Cambridge CB3 0HE, UK
‡ Toshiba Cambridge Research Centre, 260 Cambridge Science Park, Milton Road, Cambridge CB4 4WE, UK

Received 5 March 1993, in final form 6 August 1993

Abstract. Measurements of the thermopower of a one-dimensional (1D) ballistic constriction are presented and fitted by calculations for a constriction where the local potential at the bottleneck forms a saddle. The calculations show that the thermopower can be well approximated by a linear-response formulation far outside its normal range of applicability, provided that an appropriate average temperature is assumed. The fits give a saddle parameter of $\omega_y/\omega_x \geqslant 2$, which sets an upper limit of 2.2 meV on the 1D sub-band spacing.

1. Introduction

A split-gate-defined, one-dimensional (1D) constriction [1] will exhibit quantized electrical conductance G, at multiples of $2e^2/h$, when the transport is ballistic [2, 3]. In this regime, the Landauer–Büttiker formalism [4] may be used to calculate G, given the energy (E)-dependent transmission probability $t(E)$ of electrons through the constriction. This problem has been treated theoretically by several workers by calculating $t(E)$ either for sharp [5] or smoothly curved [6] constrictions, and assuming a hard-wall potential. Büttiker [7] pointed out that a more realistic model for the bottleneck of the constriction was a saddle-shaped potential, and that the appropriate $t(E)$ was already known [8]. An extension of this model to the non-linear regime [9] has been used to explain the evolution of half plateaux in G as a function of applied voltage bias [10].

An alternative way to study the transmission probability is via the thermopower S. Provided that $t(E)$ varies sufficiently slowly on an energy scale comparable to $k_B T$, which is often the case for a split-gate defined constriction, the thermopower is proportional to the energy derivative of $t(E)$. Since the electrical conductance is directly proportional to $t(E)$ at zero temperature T, this makes the thermopower a more sensitive probe of the transmission probability. Sivan and Imry [11] and Butcher [12] extended the Landauer–Büttiker formalism to account for thermal as well as electrical-potential gradients, and this approach was used by Streda [13] to calculate the thermopower of a 1D constriction assuming a step-function $t(E)$. The thermopower of a saddle-shaped potential was first considered by Proetto [14]. Here we extend these calculations to the non-linear regime, allowing for large temperature gradients, and compare with our experimental results.

§ Present address: Consejo Superior de Investigaciones Cientificas, Universidad Autonoma, E-28 049, Madrid, Spain.

0953-8984/93/438055+10$07.50

The first measurement of 1D ballistic thermopower was made by Molenkamp *et al* [15], and these results have been discussed [16] with reference to a saddle-shaped potential. Although an attempt was made to obtain more detailed quantitative results [17], we have found no convincing fit with theory in the literature. In this paper we present thermopower measurements of a 1D constriction as a function of applied temperature difference ΔT. Such a device has recently been used by the authors to demonstrate an oscillatory thermopower in the Coulomb-blockade regime [18].

This paper is organized as follows. In section 2 the theoretical predictions for the electrical conductance and thermopower of a saddle-shaped constriction are presented. Firstly the linear response predictions are discussed and then the theory is extended to account for non-linear behaviour, since all of our experimental results are in the non-linear regime. In section 3 the results are presented and in section 4 these are analysed in terms of the theory of section 2. By fitting the data with our calculations we have obtained values for the saddle-shape parameters, including an estimate of the 1D sub-band spacing in the constriction. A brief summary is given section 5.

2. Theory

The electrical current I flowing from an electron reservoir with electrochemical potential μ_1 and temperature T_1, to a second reservoir with values μ_2 and T_2, via a constriction with a transmission probability $t(E)$, is given by [11]

$$I(\mu_2; \mu_1, T_2, T_1) = -\frac{2e}{h}\int_0^\infty t(E)[f(E; \mu_1, T_1) - f(E; \mu_2, T_2)]\,\mathrm{d}E \qquad (1)$$

where f is the Fermi–Dirac function, given by

$$f(E) = \{\exp[(E-\mu)/k_\mathrm{B}T] + 1\}^{-1}. \qquad (2)$$

Defining $\Delta\mu = (\mu_2 - \mu_1)$ and $\Delta T = (T_2 - T_1)$, the conditions for linear response are $\Delta\mu,\ k_\mathrm{B}\Delta T \ll k_\mathrm{B}T_\mathrm{av}$, where $T_\mathrm{av} \equiv (T_1 + T_2)/2$ is the average temperature of the reservoirs. In this regime the zero-temperature electrical conductance $G(\mu, 0)$, as a function of the mean electrochemical potential μ, is [4]

$$G(\mu, 0) = (2e^2/h)t(\mu) \qquad (3)$$

while the thermopower is given by [11]

$$S(\mu, T) \equiv \frac{\Delta\mu}{e\Delta T} = -\frac{k_\mathrm{B}}{e}\int_{-\infty}^{+\infty}\mathrm{d}E\left(-\frac{\mathrm{d}f}{\mathrm{d}E}\right)t(E)\left(\frac{E-\mu}{k_\mathrm{B}T}\right)\Bigg/\int_{-\infty}^{+\infty}\mathrm{d}E\left(-\frac{\mathrm{d}f}{\mathrm{d}E}\right)t(E). \qquad (4)$$

We now consider the transmission probability $t(E)$ for a 1D constriction. Büttiker [7] suggested that the appropriate potential distribution $V(x, y)$ in the plane of the two-dimensional electron gas (2DEG) below a split-gate should be saddle-shaped and given by

$$V(x, y) = V_0(\mu_1, \mu_2) - \tfrac{1}{2}m\omega_x^2x^2 + \tfrac{1}{2}m\omega_y^2y^2. \qquad (5)$$

Here $V_0(\mu_1, \mu_2)$ is the electrostatic potential at the saddle point, and the curvatures of the potential are expressed in terms of the frequencies ω_x and ω_y. The Hamiltonian is

then separable into the transverse wavefunctions (1D sub-bands) associated with energies $\hbar\omega_y(i+\frac{1}{2})$, $i = 0, 1, 2, \ldots$, and a wavefunction for motion along x, in an effective potential $V_0 + \hbar\omega_y(i+\frac{1}{2}) - \frac{1}{2}m\omega_x^2 x^2$. The transmission probabilities T_{ij} from incident channel i to out-going channel j are then [7]

$$T_{ij} = \delta_{ij}/[1 + \exp(-\pi\varepsilon_i)] \tag{6a}$$

where

$$\varepsilon_i = 2[E - \hbar\omega_y(i+\tfrac{1}{2}) - V_0(\mu_1, \mu_2)]/\hbar\omega_x \tag{6b}$$

is dimensionless, and represents the excess energy in the ith 1D channel at the saddle point. When $\varepsilon_i < 0$, transport in this channel is by tunnelling. Because the Hamiltonian resulting from the potential of (5) is separable, there is no channel mixing [7], and the total transmission probability is given simply by $t(E) = \sum_i T_{ii}(E)$.

For a given value of the saddle parameter ω_y/ω_x, (3)–(6) can be used to generate both G and S as a function of the reduced electrochemical potential $(\mu_1 - V_0)/\hbar\omega_y$. In figure 1(a) the zero-temperature electrical conductance $G(\mu, 0)$ is plotted for $\omega_y/\omega_x = 3$, while in figure 1(b) the full curve represents the corresponding linear-response thermopower at a temperature of $k_B T = 0.1\hbar\omega_y$. The thermopower exhibits a peak when the electrical conductance is in a transition region between quantized plateaux, as originally predicted for a step-function $t(E)$ by Streda [13].

In the non-linear regime (4) does not apply, but given μ_1, T_1 and T_2, together with $t(E)$ from (6), we can solve (1) numerically for $I(\mu_2; \mu_1, T_1, T_2) = 0$ to obtain μ_2, and hence, $S \equiv \Delta\mu/e\Delta T$. In these calculations we make the approximation $V_0(\mu_1, \mu_2) = V_0 + \beta(\mu_2 - \mu_1)$, where β is an adjustable parameter, as previously used [9] to explain high-DC-bias results [10]. The most significant result of the calculations is that, in the case of a saddle-shaped potential, (4) is a good approximation to the thermopower well beyond the linear-response regime, provided that we set $T = T_{av}$. Given that S is linear in T for $k_B T \ll \hbar\omega_x$ [14], it is to be expected that the non-linear thermopower will lie somewhere between $S(T_1)$ and $S(T_2)$; however it is surprising that (4) is such a good approximation over a wide range of parameters, as we shall now see.

In figure 1(b) we plot the linear-response thermopower of (4), with $t(E)$ given by (6), $k_B T = 0.1\hbar\omega_y$ and $\omega_y/\omega_x = 3$. Also plotted is the thermopower calculated from (1) for $k_B T_{av} = 0.1\hbar\omega_y$ and $\omega_y/\omega_x = 3$, but with large temperature differences of $\Delta T = 0.67T_{av}(T_1 = 2T_2)$ and $\Delta T = 1.67T_{av}(T_1 = 11T_2)$. For $T_1 = 2T_2$, the linear-response approximation is always within 10% of the exact result, and even at $T_1 = 11T_2$ the discrepancy only reaches 35% at the final minimum. Here we have set $\beta = \frac{1}{2}$, as used elsewhere [9, 10]; however, further calculations show that choosing a different value for β only has the effect of shifting the curves slightly on the energy axis.

The accuracy of the linear-response approximation to the true thermopower is also largely unaffected by the choice of the saddle-shape parameter ω_y/ω_x. We have compared the results for values as large as $\omega_y/\omega_x = 6$ and find similar agreement to that demonstrated in figure 1(b). In figure 1(c) we plot S calculated from (1) with $\omega_y/\omega_x = 1.5$, and one reservoir held at a constant temperature of $k_B T_2 = 0.02\hbar\omega_y$ while T_1 is varied, in analogy with the experimental situation to be described in section 3. Again, we plot the linear-response results at the corresponding T_{av} for comparison, finding a significant discrepancy only when $k_B T_1$ becomes comparable to the 1D sub-band energy spacing $\hbar\omega_y$. Increasing the temperature has two effects on S: (i) the peaks become less distinct; and (ii) the absolute value increases, since S is approximately linearly dependent on T.

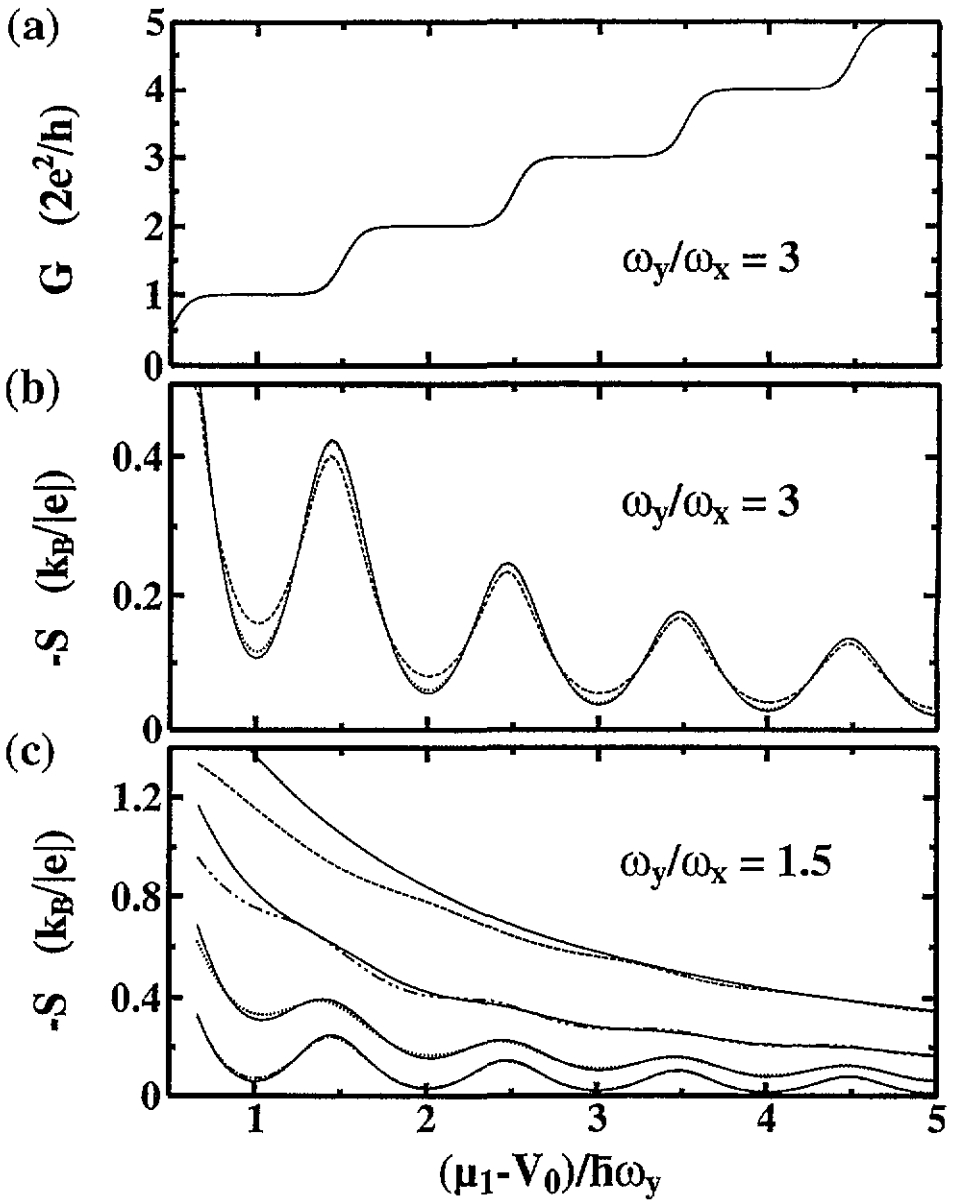

Figure 1. (a) G as a function of electrochemical potential μ_1 for $T = 0$, calculated using (3) and (6) with $\omega_y/\omega_x = 3$. (b) S calculated using the linear-response expression (full curve) of (4), and from (1) for the non-linear cases of $T_1 = 2T_2$ (dotted curve) and $T_1 = 11T_2$ (broken curve). In all three cases $\omega_y/\omega_x = 3$, and the average temperature is constant at $k_B T_{av} = 0.1\hbar\omega_y$. (c) S calculated for $\omega_y/\omega_x = 1.5$ using (1), with $k_B T_2 = 0.02\hbar\omega_y$, and with $k_B T_1/\hbar\omega_y = 0.10$ (chain curve), 0.25 (dotted curve), 0.51 (double-chain curve) and 1.05 (broken curve). The full curves are the linear-response estimates of (4) at the corresponding average temperatures: $k_B T_{av}/\hbar\omega_y = 0.06$, 0.13, 0.27 and 0.53.

3. Experimental results

The experiments were performed on a device consisting of two pairs of gold Schottky split gates (G1 and G2 in figure 2(b)), which were used to electrostatically define conducting regions in the 2DEG of a GaAs–$Al_{0.3}Ga_{0.7}As$ heterojunction. The carrier density and mobility of the 2DEG were measured at 4.2 K using a large Hall-bar device of the same material. The values obtained were 3.9×10^{15} m^{-2} and 200 m^2 V^{-1} s^{-1} respectively, implying a Fermi energy $E_F = 13$ meV, and a mean free path $l = 21$ μm. Electron-beam lithography was used to fabricate the split gates, each of which had a length of 0.3 μm and a width of 0.5 μm.

Thermoelectric measurements were made by passing a DC current I_{DC} along the central channel, of width 5 μm, in order to increase the electron temperature T_e in this region above the lattice temperature T_L (see inset in figure 2(b)). The large regions of 2DEG outside the channel were assumed to act as electron reservoirs at T_L, which was maintained at $T_L = 550$ mK by placing the sample above the liquid in a pumped He^3 system. The temperature difference $\Delta T = (T_e - T_L)$ between the central channel and the left-hand reservoir produces an electrochemical potential difference across the 1D constriction defined by gate G1, proportional to its thermopower S_1. The measured thermoelectric DC voltage $\Delta V_{th} = (V_1 - V_2)$ is then given by $\Delta V_{th} = (S_1 - S_2)\Delta T$. A small, constant offset of $S_2 \Delta T$, due to the thermopower (S_2) of G2, is always present, as discussed in [15]. Electrical conductances were measured using standard low-frequency AC techniques.

The thermoelectric and electrical conductance results obtained from split gate G1 are displayed in figure 2. In figure 2(b) we plot ΔV_{th} for various values of heating current I_{DC}, and observe peaks when G is between quantized plateaux, as first observed by Molenkamp *et al* [15]. To obtain an estimate of the ΔT produced by the various I_{DC}, the quality of the plateaux in G was used as a calibration for temperature. Over the range 2 K $< T_L <$ 15 K, the plateaux in G broadened and eventually disappeared. Similar behaviour was observed when T_L was held constant at 2 K, and I_{DC} was increased. Assuming that G, like S, is only dependent on the average temperature of the reservoirs, we compared the width of the plateaux from the two dependences to obtain T_{av} as a function of I_{DC}. We found an approximately linear relation between T_{av} and $|I_{DC}|$, as shown in the inset of figure 3. Using the relation $T_{av} = T_L + \Delta T/2$, the magnitudes of the peaks in $-\Delta V_{th}$ from figure 2(b) could then be plotted as a function of ΔT (see figure 3). Since the ΔT for these data far exceeds T_L, the measurement is well beyond linear response, as confirmed by the non-linear form of the data in figure 3. Fortunately it is still valid to calculate S using (4), provided that we set $T = T_{av}$ as discussed in section 2. This explicit expression could then be used to fit to the non-linear thermovoltage data of figure 2(b).

4. Data analysis

To gain an initial estimate of the quantization parameter ω_y/ω_x, $G(\mu)$ was calculated using (3) and compared with the data obtained at $I_{DC} = 0$. Since the plateaux in G were found to be equally spaced in gate voltage V_{g1}, it was possible to convert V_{g1} into a dimensionless energy by identifying the centres of the plateaux as corresponding to integer values of $(\mu - V_0)/\hbar\omega_y$. In figure 2(a) the data are plotted together with $G(\mu)$ calculated for $\omega_y/\omega_x = 1.0$ and 3. We have assumed here that $k_B T_L \ll \hbar\omega_y$, as justified by the thermopower results below, so that the $T = 0$ estimate of G can be used. The data exhibit clear deviations from theory; however, we obtain a best fit of $\omega_y/\omega_x = 1.7$, and a possible range of $1.0 < \omega_y/\omega_x < 3$.

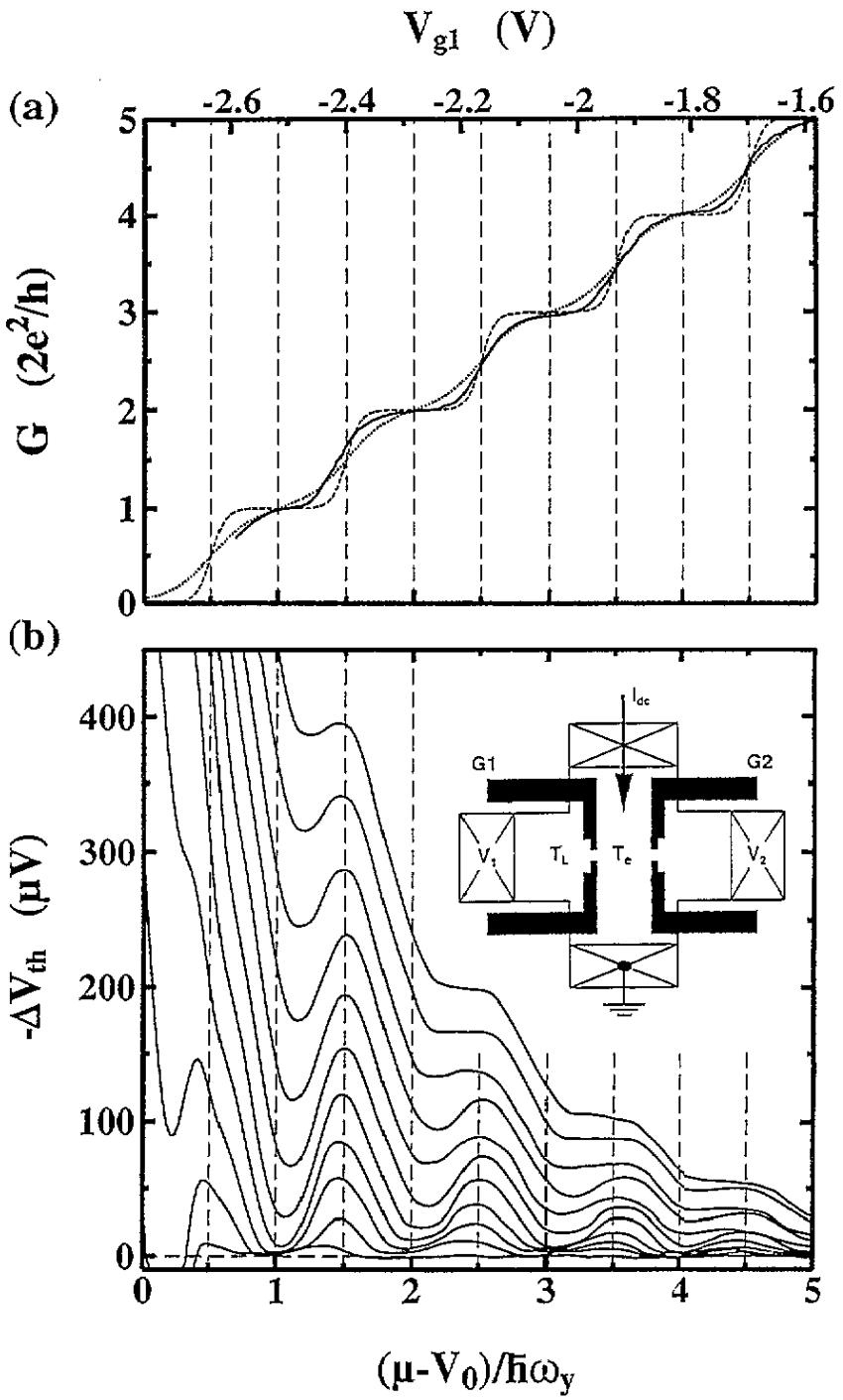

Figure 2. (a) Experimental electrical conductance G (full curve) of split-gate G1 as a function of gate voltage V_{g1} (top scale), and inferred chemical potential $(\mu - V_0)/\hbar\omega_y$ at the saddle point (bottom scale), for $I_{DC} = 0$, $T_L = 550$ mK and with a gate voltage on G2 of $V_{g2} = -2.25$ V. Also plotted is $G(\mu)$, calculated using (3) and (6), with $\omega_y/\omega_x = 1.0$ (dotted curve) and 3.0 (broken curve). (b) Measured thermoelectric voltage ΔV_{th} as a function of V_{g1} for (from the bottom): $I_{DC} = 0, 0.5, 1.0, \ldots, 5.0$ μA. Inset: Schematic of the device (not to scale), showing the two split-gates (black) used to define the heating channel.

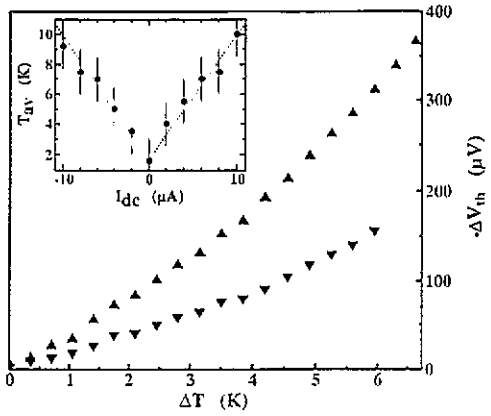

Figure 3. Peak values of $-\Delta V_{th}$ from figure 2(b), plotted as a function of ΔT, for the peaks corresponding to $(\mu - V_0)/\hbar\omega_y = 1.5$ (▲) and 2.5 (▼). Inset: The effective average temperature T_{av} at the split-gate constriction as a result of passing a current I_{DC} along the heating channel. The T_{av} values were obtained by measuring the rise in lattice temperature required to produce an amount of broadening in the electrical conductance plateaux comparable to that produced by the current I_{DC}.

Because of the convenient form of (4), and its close approximation to the exact result of (1), we have used it to fit to the thermoelectric data of figure 2(b), with the three adjustable parameters ω_y/ω_x, T_{av} and ΔT. In figure 4 we plot the measured values of $\Delta V_{th} = S_1 \Delta T$ at $I_{DC} = 3.0$ μA, together with the linear-response estimate $S(\mu, k_B T_{av})$ calculated for $\omega_y/\omega_x = 1.5$ at a variety of temperatures, and scaled to coincide with the $i = 1$ peak. Clearly, $k_B T_{av}/\hbar\omega_y = 0.11$ is the best fit to the data. The $i = 1$ peak corresponds to the transition from one- to two-channel transport, and we have chosen to fit to this peak only. For $i > 1$, the magnitude and sharpness of the peaks were always lower than predicted by theory (see figure 4). This may be due to a distortion of the parabolic potential by the higher charge densities present, or to the increase of inter-sub-band scattering as more 1D sub-bands become accessible.

Once T_{av} has been determined from the shape of the peak, ΔT may be obtained from the magnitude, via the relation $\Delta V_{th} = S\Delta T$. The best-fit values of ΔT are plotted as a function of I_{DC} in figure 5(a) for various values of ω_y/ω_x. For $\omega_y/\omega_x \geqslant 2$ we find that ΔT tends to zero with I_{DC} as expected, whereas the estimate $\omega_y/\omega_x = 1.5$ leads to unrealistically high values of ΔT near $I_{DC} = 0$. We therefore conclude that $\omega_y/\omega_x = 2$ is a lower limit for the quantization parameter. The broken line in figure 5(a) represents the dependence $\Delta T/|I_{DC}| \simeq 1.7$ K μA^{-1}, obtained from the dependence of the electrical conductance plateaux upon temperature, and corresponds to the data in the inset of figure 3. The values of ΔT obtained from the two types of measurement show good agreement, although we note that the inherent difficulties in comparing the plateaux widths limit the accuracy of that technique to only about ±20%.

In figure 5(b) we plot the best-fit values of $k_B T_{av}/\hbar\omega_y$ against ΔT, for various values of I_{DC} and ω_y/ω_x, and find an approximately linear dependence satisfying $T_{av} = T_L + \alpha\Delta T$. The gradient and intercept of the data in figure 5(b) provide values for α and $kT_L/\hbar\omega_y$, respectively. The data based on the estimate $\omega_y/\omega_x = 1.5$ has a negative intercept, indicating that $T_L < 0$, and so this estimate is too low. With $\omega_y/\omega_x = 2$, we obtain $\hbar\omega_y = (2.2 \pm 1.0)$ meV and $\alpha = 0.4 \pm 0.3$, whereas $\omega_y/\omega_x \geqslant 3$ gives $\hbar\omega_y = (0.78 \pm 0.17)$ meV

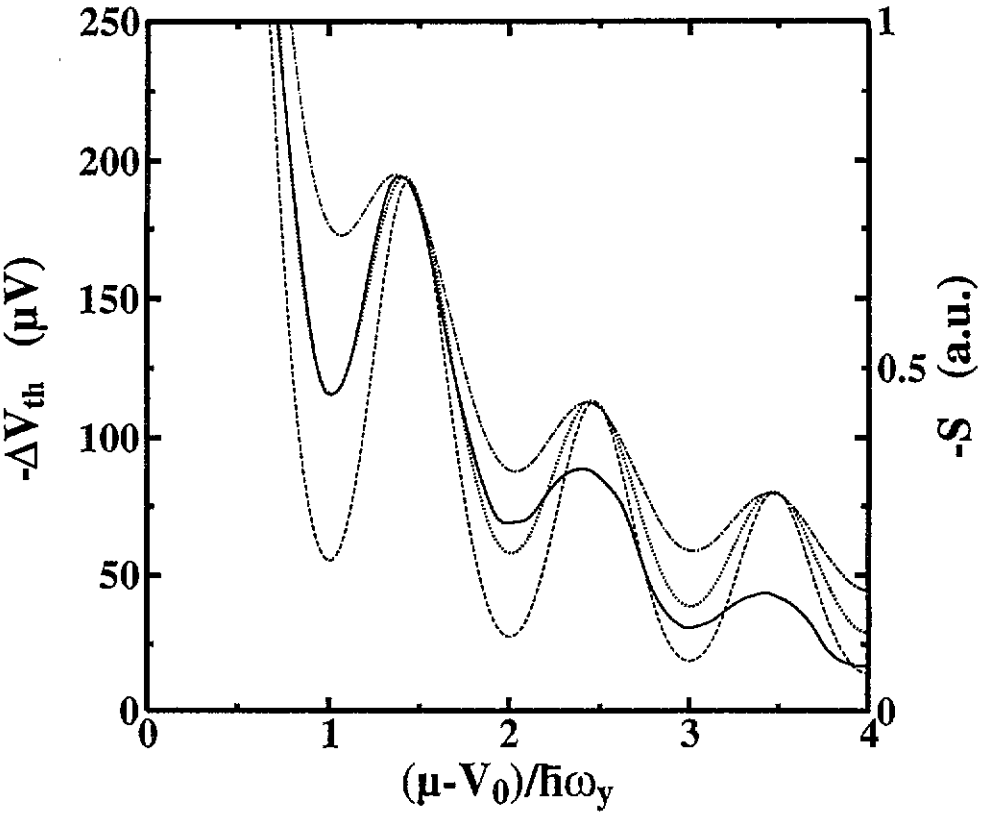

Figure 4. Measured ΔV_{th} as a function of $(\mu - V_0)/\hbar\omega_y$ for $I_{DC} = 3.0$ μA (full curve), and S calculated using (4), with $\omega_y/\omega_x = 1.5$ and $k_B T_{av}/\hbar\omega_y = 0.07$ (broken curve), 0.11 (dotted curve), and 0.15 (chain curve). The calculated curves have been scaled to coincide with the $i = 1$ peak of the data.

and $\alpha = 0.15 \pm 0.06$. In all cases we have used the known value of $T_L = 0.55$ K. Note that there is little variation in the results for values of $\omega_y/\omega_x > 3$, since when $k_B T_{av}/\hbar\omega_y \geqslant 0.1$ the width of the thermopower peak is dominated by the energy spread of (df/dE) in (4), and is relatively insensitive to the exact details of the saddle potential.

Our calculations showed that if we set $T = T_{av}$, the linear-response result is a good approximation to S, implying $\alpha = \frac{1}{2}$. The estimate $\omega_y/\omega_x = 2$ gives an α consistent with this, whereas the value obtained with $\omega_y/\omega_x = 3$ is too small, indicating that the quantization parameter is closer to $\omega_y/\omega_x = 2$. The corresponding 1D sub-band separation of $\hbar\omega_y = (2.2 \pm 1.0)$ meV is consistent with values obtained by Patel *et al* [10] from non-linear electrical conductance measurements.

5. Conclusions

In summary, DC current heating has been used to produce large temperature differences across a 1D ballistic constriction, and the resulting thermoelectric voltages have been measured. The thermopower of a constriction where the local potential at the bottleneck forms a saddle was calculated in the non-linear regime, for $\Delta T \simeq T$, and it was shown that

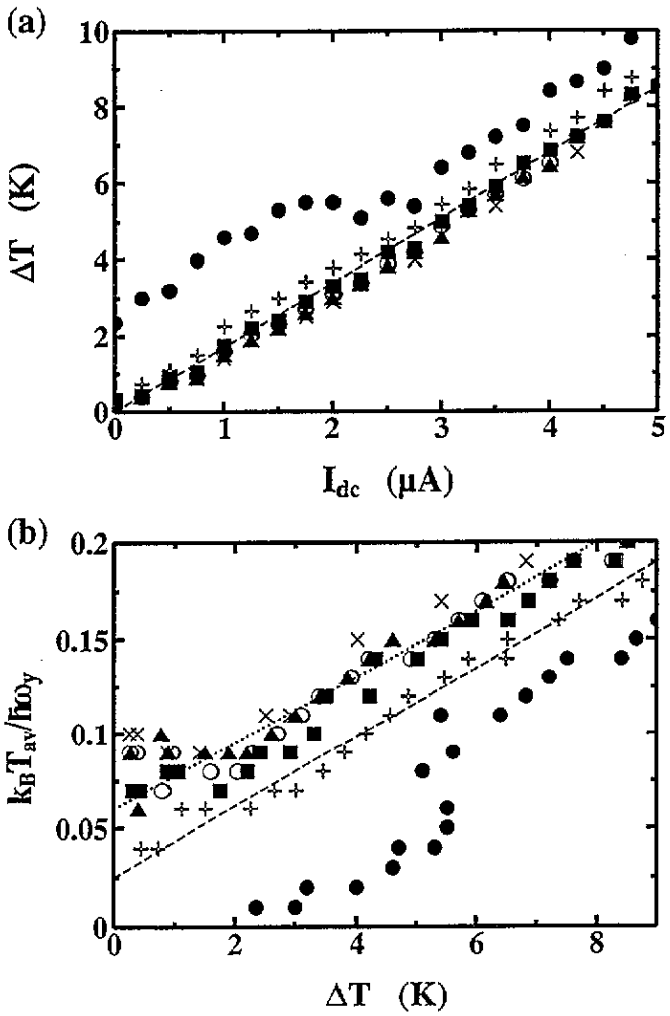

Figure 5. (a) ΔT as a function of I_{DC}, calculated by fitting (4) to the data of figure 2(b), with $\omega_y/\omega_x = 1.5$ (●), 2 (+), 3 (■), 4 (○), 5 (▲) and 30 (×). The broken line was obtained from the dependence of G upon T_L, as explained in the text. (b) Best-fit values of $k_BT/\hbar\omega_y$, plotted against ΔT for the same data, and the best-fit linear dependences for $\omega_y/\omega_x = 2$ (broken line) and $\omega_y/\omega_x \geqslant 3$ (dotted line).

a linear-response formulation was a good approximation to this result, provided that T was set to the average temperature of the reservoirs. By fitting the linear-response approximation to our data we were able to obtain values for the saddle-shape parameters, including a 1D sub-band energy separation of (2.2 ± 1.0) meV.

Acknowledgments

We thank D H Cobden, C J B Ford and A R Hamilton for helpful discussions. This work was supported by the UK Science and Engineering Research Council.

References

[1] Thornton T J, Pepper M, Ahmed H, Andrews D and Davies G J 1986 *Phys. Rev. Lett.* **56** 1198

[2] Wharam D A, Thornton T J, Newbury R, Pepper M, Ahmed H, Frost J E F, Hasko D G, Ritchie D A and Jones G A C 1988 *J. Phys. C: Solid State Phys.* **21** L209

[3] van Wees B J, van Houten H, Beenakker C W J, Williamson J G, Kouwenhoven L P, van der Marel D and Foxon C T 1988 *Phys. Rev. Lett.* **60** 848

[4] Landauer R 1957 *IBM J. Res. Dev.* **1** 223
Büttiker M 1986 *Phys. Rev. Lett.* **57** 1761

[5] Kirczenow G 1988 *Solid State Commun.* **68** 715
Szafer A and Stone A D 1989 *Phys. Rev. Lett.* **62** 300
Haanappel E G and van der Marel D 1989 *Phys. Rev.* B **39** 5484
Avishai Y and Band Y B 1989 *Phys. Rev.* B **40** 3429

[6] Glazman L I, Lesovik G B, Khmelnitskii D E and Shekhter R I 1988 *Pis. Zh. Eksp. Teor. Fiz.* **48** 218 (Engl. Transl. *JETP Lett.* **48** 239)

[7] Büttiker M 1990 *Phys. Rev.* B **41** 7906

[8] Connor J N L 1968 *Mol. Phys.* **15** 37; Miller W H 1968 *J. Chem. Phys.* **48** 1651

[9] Martín-Moreno L, Nicholls J T, Patel N K and Pepper M 1992 *J. Phys.: Condens. Matter* **4** 1323

[10] Patel N K, Nicholls J T, Martín-Moreno L, Pepper M, Frost J E F, Ritchie D A and Jones G A C 1991 *Phys. Rev.* B **44** 13549; *Phys. Rev.* B **44** 10973

[11] Sivan U and Imry Y 1986 *Phys. Rev.* B **33** 551

[12] Butcher P N 1990 *J. Phys. C: Solid State Phys.* **2** 4869

[13] Streda P 1989 *J. Phys. C: Solid State Phys.* **1** 1025

[14] Proetto C R 1991 *Phys. Rev.* B **44** 9096

[15] Molenkamp L W, van Houten H, Beenakker C W J, Eppenga R and Foxon C T 1990 *Phys. Rev. Lett.* **65** 1052

[16] van Houten H, Molenkamp L W, Beenakker C W J and Foxon C T 1992 *Semicond. Sci. Technol.* **7** B215

[17] Yamada S and Yamamoto M 1992 *Semicond. Sci. Technol.* **7** B289

[18] Dzurak A S, Smith C G, Pepper M, Ritchie D A, Frost J E F, Jones G A C and Hasko D G 1993 *Solid State Commun.* **87** 1145